DENTAL MATERIALS 35 (2019) 169–175

Available online at www.sciencedirect.com

ScienceDirect

journal homepage: www.intl.elsevierhealth.com/journals/dema

Optimal sandblasting conditions for conventional-type yttria-stabilized tetragonal zirconia polycrystals

Masahiro Okada[a], *Hiroaki Taketa*[b], *Yasuhiro Torii*[b], *Masao Irie*[a], *Takuya Matsumoto*[a,*]

[a] *Department of Biomaterials, Graduate School of Medicine, Dentistry and Pharmaceutical Sciences, Okayama University, 2-5-1 Shikata-cho, Kita-ku, Okayama 700-8558, Japan*

[b] *Department of Comprehensive Dentistry, Okayama University Hospital, 2-5-1 Shikata-cho, Kita-ku, Okayama 700-8558, Japan*

ARTICLE INFO

Article history:
Received 27 May 2018
Received in revised form
17 October 2018
Accepted 12 November 2018

Keywords:
Yttria-stabilized tetragonal zirconia polycrystals
Biaxial strength
Grinding
Sandblasting
Surface roughness

ABSTRACT

Objective. To assess the influence of sandblasting conditions applied to conventional-type yttria-stabilized tetragonal zirconia polycrystal (Y-TZP) on surface roughness, phase transformation, and biaxial flexural strength.

Methods. Commercially available Y-TZP (Lava Frame, 3M Dental Products) disks were used after sintering (specimen dimensions: 14 mm in diameter and 1.2 mm in thickness). The surfaces of specimens were ground, and then sandblast treatments were conducted at different pressures (0.20, 0.25, 0.30, 0.35 and 0.40 MPa) and distances (1, 5, 10 and 20 mm) with 50 μm alumina particles. Surface roughness measurements were performed and scanning electron microscopy (SEM) images were taken for surface characterizations. Phase transformation of Y-TZP was identified by X-ray diffraction (XRD). Biaxial flexural strength was measured using the piston-on-three-ball test.

Results. The surface roughness increased significantly by increasing the sandblasting pressure, and microcracks were observed at high sandblasting pressure at 0.40 MPa. The shortest sandblasting distance (1 mm) was not effective to increase the surface roughness compared with other sandblasting distances. A tetragonal to monoclinic phase transformation was observed after grinding. The degree of the phase transformation tended to increase with sandblasting pressure, and significant effect was independent of the sandblasting distance. The biaxial flexural test showed improved mechanical strengths for the samples after sandblasting at 0.20–0.35 MPa, with the maximum strength at 0.25 MPa. Sandblasting at 0.40 MPa decreased the strength as compared with 0.25 MPa.

Significance. The surface roughness increased with increasing the sandblasting pressure, whereas there was an optimal sandblasting pressure range to increase biaxial flexural strength of Y-TZP.

* *Corresponding author.*
E-mail address: tmatsu@md.okayama-u.ac.jp (T. Matsumoto).

https://doi.org/10.1016/j.dental.2018.11.009

1. Introduction

Zirconia-based ceramics, especially conventional yttria-stabilized tetragonal zirconia polycrystals (Y-TZP), have attracted great interest in prosthetic and implant dentistry because of their superior mechanical performance [1–3]. The mechanical performance of Y-TZP relates to the tolerance to damage under tensile stress through the crystal phase transformation from tetragonal to monoclinic phases, accompanying with 3–4% volume expansion that induces compressive stresses, closes crack tips and thus prevents further crack propagation [4,5].

The major clinical problem with the use of zirconia-based ceramics is the difficulty in achieving suitable bonding with intended synthetic substrates or natural tissues [6–8]. Airborne-particle abrasion (mainly sandblasting with alumina particles) is commonly employed, as this procedure cleans the ceramic surface, removes impurities, increases surface roughness, and modifies the surface energy and wettability [9,10], The positive effects of sandblasting on bonding between zirconia and luting agents have been evaluated by several meta-analyses [11,12], whereas the effectiveness for bonding to veneering ceramics remain unclear [13]. Moreover, the effects of sandblasting on the mechanical properties of dental zirconia remain also unclear; for example, sandblasting on Y-TZP has been reported to both increase and decrease its mechanical strength [10,14], suggesting that there is an optimal sandblasting condition to increase its mechanical strength.

In this study, in order to reveal the optimal sandblasting condition to increase mechanical strength of Y-TZP, we measured the biaxial flexural strength of commercially-available conventional Y-TZP (Lava Frame Zirconia; 3M Dental Products) after sintering, grinding, and sandblasting at different conditions (pressures at 0.20, 0.25, 0.30, 0.35 or 0.40 MPa, and distances of 1, 5, 10 or 20 mm). The effects of sandblasting condition on surface roughness and crystalline phase of Y-TZP are also reported. The null hypothesis is that there is no difference between the biaxial flexural strengths of Y-TZP after sandblasting at different conditions.

2. Materials and Methods

2.1. Materials

Pre-sintered Y-TZP (Lava Frame Zirconia) was kindly donated by 3M Dental Products (Seefeld, Germany). Alumina particles with 50 μm in size (Hi-Aluminas; Shofu Inc., Kyoto, Japan) were used for sandblasting.

2.2. Sample preparation

A low-speed cutting machine was used to cut the pre-sintered zirconia under wet conditions with tap water. After the disks were sintered at 1500 °C for 2 h (heating rate: 20 °C/min from room temperature to 800 °C; 10 °C/min from 800 °C to 1500 °C; cooling rate: below 15 °C/min), the sintered Y-TZP disks (approximately 14 mm in diameter and 1.2 mm in thickness; total number, 75) were divided randomly into the following groups:

Group A (as-sintered samples): The samples after sintering were used without any treatments.

Group G (ground samples): After sintering, both sides of the disks were ground sequentially with #120, #320, and #600 silicon carbide abrasive papers (Buehler, a division of Illinois Tool Works Inc., IL, USA) under tap water irrigation to remove pollutants. In order to standardize the grinding conditions, the grinding procedure was performed by a single operator, and each abrasive paper was exchanged after grinding one side of each disk.

Group SB (sandblasted samples): One side of each disk after grinding was sandblasted with 50 μm alumina particles using a laboratory sandblaster (Hi-Blaster III; Shofu Inc., Kyoto, Japan) for 10 s at different pressures and distances. After sandblasting, each disk was separately cleaned with water three times, where water was replaced each time, in an ultrasonic cleaner (ASU-2D; AS ONE Corp., Osaka, Japan) for 1 min at 23 kHz to remove the alumina particles and debris. The sample names were noted as SB/x MPa/y mm (*e.g.*, SB/0.25 MPa/10 mm), where *x* and *y* indicate the sandblasting pressure and distance, respectively. In this study, the following 8 different sandblasting conditions were applied by a single operator: SB/0.20 MPa/10 mm, SB/0.25 MPa/10 mm, SB/0.30 MPa/10 mm, SB/0.35 MPa/10 mm, SB/0.40 MPa/10 mm, SB/0.25 MPa/1 mm, SB/0.25 MPa/15 mm, and SB/0.25 MPa/20 mm.

2.3. Biaxial flexural strengths

The biaxial flexural strength test (N = 5) was performed using the piston-on-three ball technique [15] in a universal testing machine (Autograph AG-X, Shimadzu Corp., Kyoto, Japan). Three 3.2 mm diameter stainless steel balls that were equidistant from each other were placed on a circle with a diameter of 10 mm. The disk was placed centrally on the steel balls. Unless otherwise stated, the sandblasted side faced the steel balls, where a load piston (1.2 mm in diameter) was applied from the side opposite to sandblasted surface (crosshead speed of 1.0 mm/min) in order to apply a tensile stress on the sandblasted side. The fracture load for each specimen was recorded, and the biaxial flexural strength was calculated using the following Eq. (1):

$$S = \frac{-0.2387\ P(X - Y)}{d^2} \quad (1)$$

where S is biaxial flexural strength (MPa); P is fracture load (N); and *d* is specimen disk thickness at fracture origin (mm). X and Y were determined as follows:

$$X = (1+u)\ln\left(\frac{r_2}{r_3}\right)^2 + \left[\frac{1-u}{2}\right]\left(\frac{r_2}{r_3}\right)^2 \quad (2)$$

$$Y = (1+u)\left[1+\ln\left(\frac{r_1}{r_3}\right)^2\right] + (1-u)\left(\frac{r_1}{r_3}\right)^2 \quad (3)$$

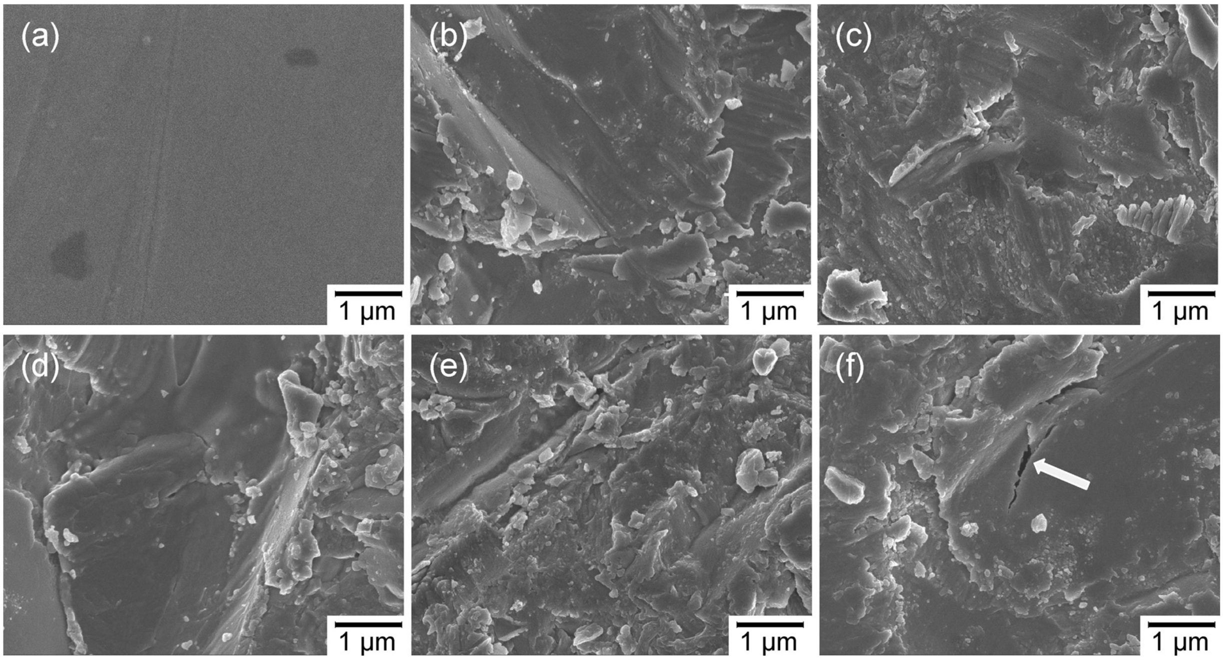

Fig. 1 – Scanning electron microscope (SEM) photographs of yttria-stabilized tetragonal zirconia polycrystal (Y-TZP) after (a: Group G) grinding and (b–f: Groups SB) sandblasting at different pressures (MPa): (b) 0.20, (c) 0.25, (d) 0.30, (e) 0.35, and (f) 0.40. The sandblasting distance was 10 mm and the time was 10 s. The white arrow indicates a microcrack.

where u is Poisson's ratio (0.25), r_1 is the radius of the support circle, r_2 is the radius of the load piston, and r_3 is the radius of the sample.

2.4. *Surface Characterizations*

The phase transformation induced by the surface treatments was determined by measuring the peak intensity ratio in the X-ray diffraction (XRD) pattern of the samples. The XRD data were collected with a $\theta/2\theta$ diffractometer (RINT2500HF) using Cu-Kα (1.54 Å) irradiation at 40 kV and 200 mA. XRD patterns were obtained in the range $2\theta = 25–36^\circ$ at a scan speed of 2°/min. Monoclinic peak intensity ratio (X_m) was calculated using the method reported by Garvie and Nicholsone [16] as follows:

$$X_m = \frac{I_m\left(\bar{1}11\right) + I_m\left(111\right)}{I_m\left(\bar{1}11\right) + I_m\left(111\right) + I_t\left(111\right)} \quad (4)$$

where I_t and I_m represent the integrated intensities of tetragonal $(111)_t$ peak and monoclinic $(111)_m$ and $(-111)_m$ peaks around $2\theta = 30^\circ$, 31° and 28°, respectively. Monoclinic phase content (F_m) was calculated using the method reported by Taraya et al. [17] as follows:

$$F_m = \frac{1.311X_m}{1 + 0.311X_m} \quad (5)$$

The surface morphology was observed by scanning electron microscopy (SEM) using a JSM-6701F microscope (JEOL Ltd., Tokyo, Japan) operated at 5 kV after each sample was fixed on an aluminum stub and coated using a Neoc-Pro osmium coater (Meiwafosis Co. Ltd., Tokyo, Japan).

The average surface roughness (Ra) of each sample was determined using a profilometer (HandySurf E-35B; Mitutoyo Corp., Kanagawa, Japan) with active tip radius of 2 μm, reading length of 1.0 mm, and reading speed of 0.6 mm/s. Five measurements at different locations, in which the distance between each parallel track set at least 0.5 mm, were recorded for each specimen, and the average value was calculated.

2.5. *Statistical analysis*

After the normality and the homogeneity of variance were tested using Shapiro-Wilk and Levene's tests, respectively, a one-way analysis of variance (ANOVA) was performed to investigate the effect of sandblasting pressure (Groups A, G, SB/0.20 MPa/10 mm, SB/0.25 MPa/10 mm, SB/0.30 MPa/10 mm, SB/0.35 MPa/10 mm, and SB/0.40 MPa/10 mm), distance (Groups SB/0.25 MPa/1 mm, SB/0.25 MPa/5 mm, SB/0.25 MPa/10 mm, and SB/0.25 MPa/20 mm), or load direction for SB/0.25 MPa/10 mm. The Tukey-Kramer test was used to detect multiple comparisons among the above experimental groups. All statistical tests were performed using R ver. 3.3.2 [18] at preset alpha levels of 0.05.

3. Results

3.1. *Sandblasting pressure*

First, the effect of sandblasting pressure was investigated using conventional Y-TZP at constant sandblasting distance (10 mm). The SEM image and the surface roughness profile of as-sintered Y-TZP (Group A) were summarized in Supplemental Fig. S1. Fig. 1 shows SEM images of the samples after the mechanical surface treatments (Groups G and SB). Before sandblasting (*i.e.*, just after grinding with silicon carbide abrasive paper under water-cooling conditions; Group G), superficial flaws such as scratches were observed. The sandblasted samples (Groups SB) showed rough surfaces, and some microcracks were formed at the highest sandblasting pressure at 0.40 MPa. As shown in Fig. 2, Ra values increased with increasing sandblasting pressure, and the largest Ra value was obtained at the highest sandblasting pressure (0.40 MPa).

Fig. 3 shows the XRD patterns of as-sintered samples (Group A) without any treatment, showing only tetragonal phase. After grinding (Group G), the broadening of the tetragonal (111) peak at $2\theta = 30°$ was observed (Fig. 3b) and the full width at half maximum (FWHM) of the peak increased from 0.18 to 0.34. In Fig. 3b, the monoclinic (−111) peak at $2\theta = 28.2°$ was detected, and the monoclinic phase content (F_m) was 2.0% after grinding (Group G). After sandblasting (Group SB), F_m and FWHM increased up to 10.3% and 0.45, respectively, by increasing the sandblasting pressures (Figs. 3c–g).

Biaxial flexural strengths before and after the mechanical surface treatments are summarized in Fig. 4. Although there is no statistically significant difference between Groups A (*i.e.*, as-sintered samples) and G (*i.e.*, the samples after grinding), Groups SB at 0.20–0.35 MPa significantly improved the flexural strength compared with Groups A and G. However, the strength decreased significantly after sandblasting at the highest pressure of 0.40 MPa compared with 0.25 MPa. Note that when the load piston was applied from side with the sandblasted surface in order to apply a compressive stress on the sandblasted side (*i.e.*, tensile stress was applied on the non-sandblasted surfaces after grinding), there was no significant different between the strengths of Group

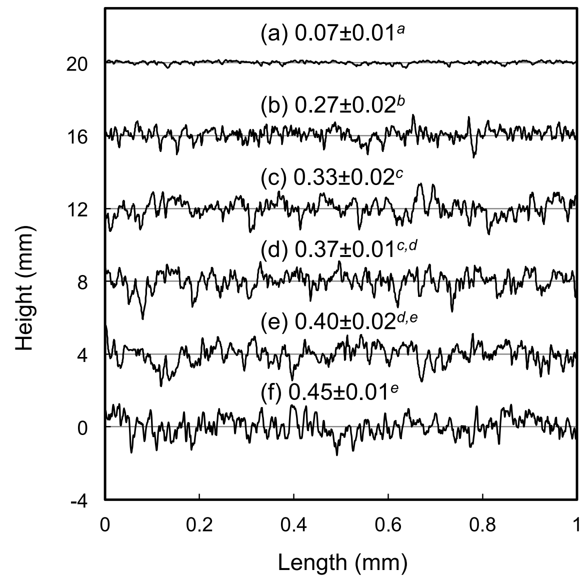

Fig. 2 – Surface roughness profiles for conventional yttria-stabilized tetragonal zirconia polycrystal (Y-TZP) after (a: Group G) grinding and (b–f: Groups SB) sandblasting at different pressures (MPa): (b) 0.20, (c) 0.25, (d) 0.30, (e) 0.35, and (f) 0.40. The sandblasting distance was 10 mm and the time was 10 s. The values indicate the calculated average roughness (Ra) value (μm) ±standard deviation (SD) (*N* = 5). Different italic superscript letters on the values indicate statistically significant difference between the groups from Tukey–Kramer tests (p < 0.05).

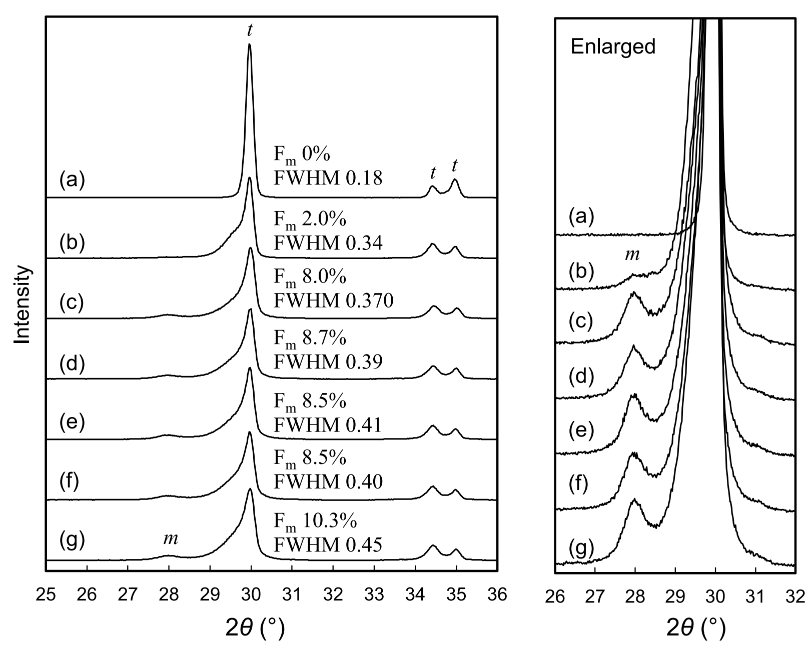

Fig. 3 – X-ray diffraction (XRD) patterns of (a: Group A) as-sintered yttria-stabilized tetragonal zirconia polycrystal (Y-TZP) and those after (b: Group G) grinding followed by (c–g: Groups SB) sandblasting at different pressures (MPa): (c) 0.20, (d) 0.25, (e) 0.30, (f) 0.35, and (g) 0.40. The sandblasting distance was 10 mm and the time was 10 s. The right graph contains enlarged XRD patterns showing monoclinic phase. *m*: monoclinic phase; *t*: tetragonal phase; F_m: monoclinic phase content; and FWHM: full width at half maximum of the peak at $2\theta = 30°$.

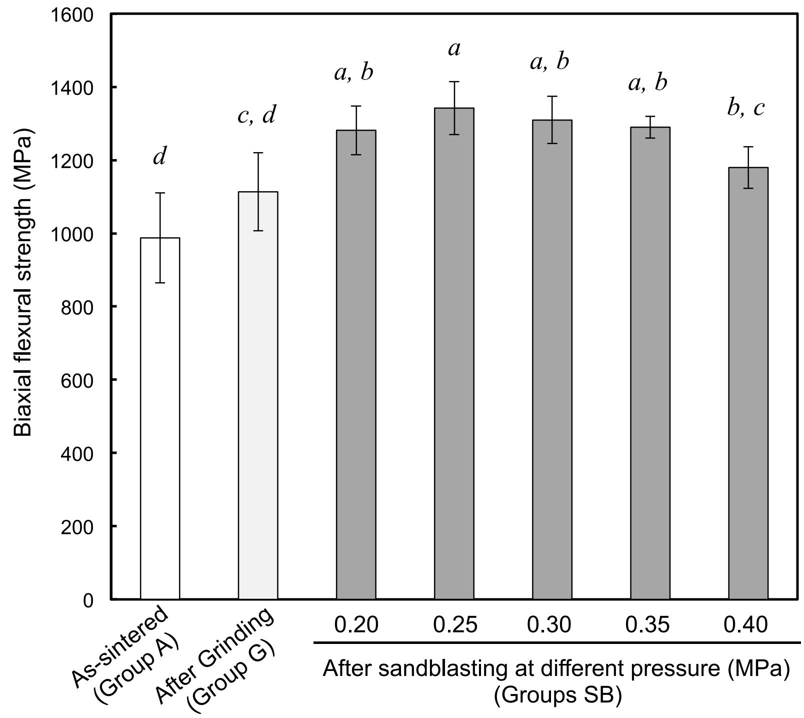

Fig. 4 – Biaxial flexural strengths of as-sintered yttria-stabilized tetragonal zirconia polycrystal (Y-TZP) and those after grinding and sandblasting at different pressures. The sandblasting distance was 10 mm and the time was 10 s. Error bars show standard deviation (SD) ($N = 5$). Different italic letters on the bars indicate statistically significant difference between the groups from Tukey-Kramer test ($p < 0.05$).

Table 1 – Monoclinic phase contents (F_m), average roughness (Ra) and biaxial flexural strengths of yttria-stabilized tetragonal zirconia polycrystal (Y-TZP) after sandblasting at 0.25 MPa at different distances. Ra and biaxial flexural strength values are given as mean ± standard deviation (SD).

Distance (mm)	1	5	10	20
F_m (%)	7.3	8.5	8.7	7.7
Ra (μm)	0.26 ± 0.06^b	0.37 ± 0.04^a	0.33 ± 0.02^a	0.38 ± 0.02^a
Biaxial flexural strength (MPa)	1380 ± 56^A	1364 ± 32^A	1342 ± 72^A	1322 ± 45^A

Different superscript letters indicate statistically significant difference between the groups from Tukey–Kramer test ($p < 0.05$).

SB/0.25 MPa/10 mm and of Group G (Supplemental Fig. S2), suggesting the formation of a surface compressive force only on the sandblasted surface.

3.1.1. *Sandblasting distances*

The effect of sandblasting distance was investigated using conventional Y-TZP at constant sandblasting pressure (0.25 MPa). The results were summarized in Table 1. Note that the sandblasting was inhomogeneous in the case of short sandblasting distances at 1 and 5 mm (Supplemental Fig. S3). At all distances in the range 1–20 mm, F_m and Ra increased by sandblasting compared with the ground samples (Group G). The Ra value for the samples after sandblasting at 1 mm distance were smaller than those at other sandblasting distances, suggesting that there remained some surface regions that had not received abrasion. However, the sandblasting distance does not significantly change the biaxial flexural strength.

4. Discussion

This study showed that there was significant difference between the biaxial flexural strengths of the sandblasted Y-TZP samples at different sandblasting pressure conditions. Therefore, the null hypothesis was rejected, and hence our results suggest that there is an optimal sandblasting condition to increase the mechanical strength of conventional Y-TZP.

In this study, the sandblasting was conduced onto the samples after grinding both sides of the samples with silicon carbide abrasive papers under a water-cooling condition, in order to reduce the variations of parallelism and flatness of the sample disks for biaxial flexural tests. Zirconia-based prostheses are prepared using a computer-aided design and computer-aided manufacturing (CAD/CAM) technology. Although the precision of CAD/CAM technology has been improved, zirconia-based prostheses require a grinding process with diamond rotary instruments in order to increase its adaptability or to adjust the occlusion during the fabrication or the clinical application stage [19]. Grinding had been recommended as a surface treatment for zirconia to improve the bond strength to veneering porcelain, although the recommendation cannot be verified by a recent systematic review [20]. In terms of the effect of grinding on mechanical properties of Y-TZP, Garvie et al. first reported the strengthening of zirconia-based ceramics after grinding due to the association between tetragonal-to-monoclinic transformation and the generation of superficial compressive stress [21]. However, grinding has also been reported to exert both positive and negative effects on Y-TZP. For example, the grinding of Y-TZP with diamond burr under dry conditions caused a significant decrease in the flexural strength [22], whereas grinding under water-cooling conditions caused a significant increase in the strength [23,24]. Our results showed that grinding with silicon carbide fixed abrasives under water-cooling conditions (Group G) did not significantly affect the biaxial strength of Y-TZP as compared with as-sintered samples (Group A). The inconsistency of the grinding effects compared with the previous studies would be due to different degrees of tetragonal phase transformation (*i.e.*, degree of superficial compressive stress generation) on Y-TZP and of superficial flaw formation. In clinical/laboratory situations, diamond-fixed/impregnated burs have been recommended for grinding due to their high grinding efficiency and low heat generation [19]. Lee et al. evaluated the effects of the components in grinding burs, and reported that the bur impregnated with silicon carbide grains induced less degree of tetragonal phase transformation of Y-TZP as compared with diamond burs [19]. Note that the tetragonal phase transformation depth (70–120 nm [19]) is much lower than the sandblasting depth (around 5 μm in the case of sandblasting with 50-μm alumina at 0.2 MPa for 7 s [25]), and the effect of grinding on mechanical properties would be negligible after sandblasting homogeneously.

The sandblast treatment involves impacting the target surface with hard particles at high velocities, thereby eroding the material and leaving a roughened surface with expected higher wettability [9]. Although there are some systematic experimental data for understanding the effects of airborne particle sizes on the mechanical properties of Y-TZP [26–28], to the best of our knowledge, there is no report on the effect of the sandblasting distance, and there are only two reports for the sandblasting pressures: Egilmez et al. [29] compared the flexural strengths of as-sintered Y-TZP and those after sandblasting at 0.2, 0.4 and 0.6 MPa with 110-μm alumina, whose size was larger than that recommended by manufacturers (*e.g.*, <50 μm [30]; 50–70 μm [31]); and Moon et al. [9] systematically compared flexural strengths of Y-TZP after polishing and after sandblasting with three different sizes of alumina particles (25, 50, and 125 μm), two different pressures (2 and 4 bar), two distinct application times (10 and 20 s) and two distinct incidence angles (45° and 90°) by using three-point bending tests that have been used extensively in the past but have a significant disadvantage in that it is difficult to eliminate undesirable edge failures [32,33] as compared with the biaxial flexural strength tests used in this study. In this study, we also showed that the surface roughness increased with increasing the sandblasting pressure, whereas there was an optimal pressure range to increase the biaxial flexural strength of Y-TZP. The sandblast treatment applied to Y-TZP surfaces have been reported to induce protective compressive residual stresses from the tetragonal-to-monoclinic transformation, thereby increasing the flexural strength [10]. However, as shown in the SEM images in this study, too much sandblasting pressure induced the formation of microcracks that decreased the flexural strength. At the optimum sandblasting pressure (0.25 MPa) in this study, although the short sandblasting distance resulted in inhomogeneous surfaces (*i.e.*, there remained some surface regions that had not received abrasion), the sandblasting distance ranging 1–20 mm does not significantly affect the biaxial flexural strength, which might be due to the limitation of in-vitro biaxial flexural strength tests (*i.e.*, it seems to be important to form protective compressive residual stresses near the fracture point). Although the sandblasting time was fixed to 10 s in this study, the sandblasting time also influenced the formation of protective compressive residual stresses [11]. Further studies will provide more optimal sandblasting conditions for Y-TZP.

5. Conclusions

Within the limitations of this study, the following conclusions were drawn:

1. After mechanical surface treatment, phase transformation of tetragonal to monoclinic was observed for conventional Y-TZP.
2. Grinding with silicone carbide fixed abrasions under water-cooling conditions did not significantly change the biaxial flexural strength of Y-TZP.
3. Sandblasting increased the surface roughness of Y-TZP.
4. There was an optimal sandblasting pressure range to improve the strength of Y-TZP, and the optimal sandblasting pressure range for Lava Frame Zirconia was 0.20–0.35 MPa in the case of sandblasting time of 10 s.

Acknowledgements

This work was supported in part by the Japan Society for the Promotion of Science KAKENHI Grant Numbers JP15K13303, JP18K09637 and JP18K17098

Appendix A. Supplementary data

Supplementary data associated with this article can be found, in the online version, at https://doi.org/10.1016/j.dental.2018.11.009.

REFERENCES

[1] Apratim A, Eachempati P, Krishnappa Salian KK, Singh V, Chhabra S, Shah S. Zirconia in dental implantology: a review. J Int Soc Prev Community Dent 2015;5:147–56, http://dx.doi.org/10.4103/2231-0762.158014.

[2] Pjetursson BE, Sailer I, Makarov NA, Zwahlen M, Thoma DS. All-ceramic or metal-ceramic tooth-supported fixed dental prostheses (FDPs)? A systematic review of the survival and complication rates. Part II: multiple-unit FDPs. Dent Mater

2015;31:624–39,
http://dx.doi.org/10.1016/j.dental.2015.02.013.
[3] Sailer I, Makarov NA, Thoma DS, Zwahlen M, Pjetursson BE. All-ceramic or metal-ceramic tooth-supported fixed dental prostheses (FDPs)? A systematic review of the survival and complication rates. Part I: single crowns (SCs). Dent Mater 2015;31:603–32,
http://dx.doi.org/10.1016/j.dental.2015.02.011.
[4] Porter DL, Heuer AH. Mechanisms of toughening Partially Stabilized Zirconia (PSZ). J Am Ceram Soc 1977;60:183–4,
http://dx.doi.org/10.1111/j.1151-2916.1977.tb15509.x.
[5] Piconi C, Maccauro G. Zirconia as a ceramic biomaterial. Biomaterials 1999;20:1–25,
http://dx.doi.org/10.1016/S0142-9612(98)00010-6.
[6] Thompson JY, Stoner BR, Piascik JR, Smith R. Adhesion/cementation to zirconia and other non-silicate ceramics: where are we now? Dent Mater 2011;27:71–82,
http://dx.doi.org/10.1016/j.dental.2010.10.022.
[7] Tzanakakis E-GC, Tzoutzas IG, Koidis PT. Is there a potential for durable adhesion to zirconia restorations? A systematic review. J Prosthet Dent 2016;115:9–19,
http://dx.doi.org/10.1016/j.prosdent.2015.09.008.
[8] Okada M, Inoue K, Irie M, Taketa H, Torii Y, Matsumoto T. Resin adhesion strengths to zirconia ceramics after primer treatment with silane coupling monomer or oligomer. Dent Mater J 2017;36:600–5,
http://dx.doi.org/10.4012/dmj.2016-334.
[9] Moon J-E, Kim S-H, Lee J-B, Han J-S, Yeo I-S, Ha S-R. Effects of airborne-particle abrasion protocol choice on the surface characteristics of monolithic zirconia materials and the shear bond strength of resin cement. Ceram Int 2016;42:1552–62,
http://dx.doi.org/10.1016/j.ceramint.2015.09.104.
[10] Aurélio IL, Maria A, Marchionatti E, Montagner AF, May LG, Soares FZM. Does air particle abrasion affect the flexural strength and phase transformation of Y-TZP? A systematic review and meta-analysis. Dent Mater 2016;32:827–58,
http://dx.doi.org/10.1016/j.dental.2016.03.021.
[11] Inokoshi M, De Munck J, Minakuchi S, Van Meerbeek B. Meta-analysis of bonding effectiveness to zirconia ceramics. J Dent Res 2014;93:329–34,
http://dx.doi.org/10.1177/0022034514524228.
[12] Özcan M, Bernasconi M. Adhesion to zirconia used for dental restorations: a systematic review and meta-analysis. J Adhes Dent 2015;17:7–26, http://dx.doi.org/10.3290/j.jad.a33525.
[13] Miyazaki T, Nakamura T, Matsumura H, Ban S, Kobayashi T. Current status of zirconia restoration. J Prosthodont Res 2013;57:236–61, http://dx.doi.org/10.1016/j.jpor.2013.09.001.
[14] Inokoshi M, Zhang F, Vanmeensel K, De Munck J, Minakuchi S, Naert I, et al. Residual compressive surface stress increases the bending strength of dental zirconia. Dent Mater 2017;33:e147–54,
http://dx.doi.org/10.1016/j.dental.2016.12.007.
[15] Wille S, Hölken I, Haidarschin G, Adelung R, Kern M. Biaxial flexural strength of new Bis-GMA/TEGDMA based composites with different fillers for dental applications. Dent Mater 2016;32:1073–8,
http://dx.doi.org/10.1016/j.dental.2016.06.009.
[16] Garvie RC, Nicholson PS. Phase analysis in zirconia systems. J Am Ceram Soc 1972;55:303–5,
http://dx.doi.org/10.1111/j.1151-2916.1972.tb11290.x.
[17] Toraya H, Yoshimura M, Somiya S. Calibration curve for quantitative analysis of the monoclinic-tetragonal ZrO_2 system by X-ray diffraction. J Am Ceram Soc 1984;67:C-119–21,
http://dx.doi.org/10.1111/j.1151-2916.1984.tb19715.x.
[18] R Development Core Team. R: a Language and Environment for Statistical Computing 2016.
[19] Lee K-R, Choe H-C, Heo Y-R, Lee J-J, Son M-K. Effect of different grinding burs on the physical properties of zirconia. J Adv Prosthodont 2016;8:137,
http://dx.doi.org/10.4047/jap.2016.8.2.137.
[20] Lundberg K, Wu L, Papia E. The effect of grinding and/or airborne-particle abrasion on the bond strength between zirconia and veneering porcelain: a systematic review. Acta Biomater Odontol Scand 2017;0:000,
http://dx.doi.org/10.1080/23337931.2017.1293486.
[21] Garvie RC, Hannink RH, Pascoe RT. Ceramic steel? Nature 1975;258:703–4, http://dx.doi.org/10.1038/258703a0.
[22] Karakoca S, Yilmaz H. Influence of surface treatments on surface roughness, phase transformation, and biaxial flexural strength of Y-TZP ceramics. J Biomed Mater Res – Part B Appl Biomater 2009;91:930–7,
http://dx.doi.org/10.1002/jbm.b.31477.
[23] Hatanaka GR, Polli GS, Fais LMG, Reis JM, dos SN, Pinelli LAP. Zirconia changes after grinding and regeneration firing. J Prosthet Dent 2017;118:61–8,
http://dx.doi.org/10.1016/j.prosdent.2016.09.026.
[24] Pereira GKR, Silvestri T, Camargo R, Rippe MP, Amaral M, Kleverlaan CJ, et al. Mechanical behavior of a Y-TZP ceramic for monolithic restorations: effect of grinding and low-temperature aging. Mater Sci Eng C 2016;63:70–7,
http://dx.doi.org/10.1016/J.MSEC. 2016.02.049.
[25] Su N, Yue L, Liao Y, Liu W, Zhang H, Li X, et al. The effect of various sandblasting conditions on surface changes of dental zirconia and shear bond strength between zirconia core and indirect composite resin. J Adv Prosthodont 2015;7:214, http://dx.doi.org/10.4047/jap.2015.7.3.214.
[26] Özcan M, Melo RM, Souza ROA, Machado JPB, Felipe Valandro L, Botttino MA. Effect of air-particle abrasion protocols on the biaxial flexural strength, surface characteristics and phase transformation of zirconia after cyclic loading. J Mech Behav Biomed Mater 2013;20:19–28,
http://dx.doi.org/10.1016/j.jmbbm.2013.01.005.
[27] Yamaguchi H, Ino S, Hamano N, Okada S, Teranaka T. Examination of bond strength and mechanical properties of Y-TZP zirconia ceramics with different surface modifications. Dent Mater J 2012;31:472–80,
http://dx.doi.org/10.4012/dmj.2011-237.
[28] Fonseca RG, De Oliveira Abi-Rached F, Maurício J, Santos D, Reis N, Rambaldi E, et al. Effect of particle size on the flexural strength and phase transformation of an airborne-particle abraded yttria-stabilized tetragonal zirconia polycrystal ceramic. J Prosthet Dent 2013;110:510–4,
http://dx.doi.org/10.1016/j.prosdent.2013.07.007.
[29] Egilmez F, Ergun G, Cekic-Nagas I, Vallittu PK, Lassila LVJ. Factors affecting the mechanical behavior of Y-TZP. J Mech Behav Biomed Mater 2014;37:78–87,
http://dx.doi.org/10.1016/j.jmbbm.2014.05.013.
[30] ESPE 3M. Lava™ Plus High Translucency Zirconia System Technical Product Profile. 2012.
[31] Kuraray Noritake Dental Inc. Katana Zirconia Technical Guide. 2017.
[32] Ritter JE, Jakus K, Batakis A, Bandyopadhyay N. Appraisal of biaxial strength testing. J Non-Cryst Solids 1980;38–39:419–24.
[33] Jin J, Takahashi H, Iwasaki N. Effect of test method on flexural strength of recent dental ceramics. Dent Mater J 2004;23:490–6.